




Article

# Revalorizing a Pyrolytic Char Residue from Post-Consumer Plastics into Activated Carbon for the Adsorption of Lead in Water

Rafael R. Solís , María Ángeles Martín-Lara \* , Ana Ligeró, Josefa Balbís, Gabriel Blázquez   
and Mónica Calero \*

Chemical Engineering Department, Faculty of Sciences, University of Granada, 18071 Granada, Spain

\* Correspondence: marianml@ugr.es (M.Á.M.-L.); mcalero@ugr.es (M.C.)

**Abstract:** This work focuses on the use of a char produced during the pyrolysis of a mixture of non-recyclable plastics as a precursor for the preparation of porous activated carbon with high developed adsorption uptake of lead in water. Physical and chemical activation was used to enhance the porosity, surface area, and surface chemistry of char. The final activated carbon materials were deeply characterized through N<sub>2</sub> adsorption isotherms, scanning electron microscopy, Fourier transformed infrared spectroscopy, analysis of the metal content by inductively coupled plasma mass spectroscopy, and pH of point zero charge. The native char displayed a Pb adsorption uptake of 348 mg Pb·g<sup>-1</sup> and considerably high leaching of carbon, mainly organic, ca. 12%. After stabilization with HCl washing and activation with basic character activators, i.e., CO<sub>2</sub>, NaOH, and KOH, more stable adsorbents were obtained, with no organic leaching and a porous developed structure, the order of activation effectiveness being KOH (487 m<sup>2</sup>·g<sup>-1</sup>) > NaOH (247 m<sup>2</sup>·g<sup>-1</sup>) > CO<sub>2</sub> (68 m<sup>2</sup>·g<sup>-1</sup>). The activation with KOH resulted in the most effective removal of Pb in water with a saturation adsorption uptake of 747 mg Pb·g<sup>-1</sup>.

**Keywords:** pyrolytic char; chemical activation; adsorption; lead; plastic waste



**Citation:** Solís, R.R.; Martín-Lara, M.Á.; Ligeró, A.; Balbís, J.; Blázquez, G.; Calero, M. Revalorizing a Pyrolytic Char Residue from Post-Consumer Plastics into Activated Carbon for the Adsorption of Lead in Water. *Appl. Sci.* **2022**, *12*, 8032. <https://doi.org/10.3390/app12168032>

Academic Editor: Bart Van der Bruggen

Received: 15 July 2022

Accepted: 10 August 2022

Published: 11 August 2022

**Publisher's Note:** MDPI stays neutral with regard to jurisdictional claims in published maps and institutional affiliations.



**Copyright:** © 2022 by the authors. Licensee MDPI, Basel, Switzerland. This article is an open access article distributed under the terms and conditions of the Creative Commons Attribution (CC BY) license (<https://creativecommons.org/licenses/by/4.0/>).

## 1. Introduction

Plastic pollution is one of the most challenging environmental hazards. The fast rate of plastic consumption and very short time of use before disposal overwhelms the ability to manage them after disposal. Currently, over 350 tons of plastics are produced by developed countries annually, and this number is expected to quadruple by 2050 due to more demand in the market [1]. Plastics frequently end up in natural ecosystems due to inadequate collection and disposal. Larger plastic debris, known as macroplastics, degrade into microplastics that pollute aquatic ecosystems, mainly oceans [2]. The recycling rates of plastic are very low even in developed countries, i.e., around 10% [3]. Furthermore, only 15–20% of all plastic waste is recycled using conventional mechanical methods such as sorting, grinding, washing, and extrusion [4]. The rest add to the burdens of landfills, filling them to their limits. Therefore, non-recyclable plastic fractions have been proposed as a source for tertiary technologies such as pyrolysis, in which polymers become lighter monomers under an inert atmosphere at high temperatures [4,5]. This technology aims at the circular management of plastics' life and transforms them into gaseous substances, liquid, and solid products [6]. The gas product can be used as an energy source to provide the energy required for the pyrolysis process. The liquid product is an important renewable material for the generation of chemicals and fuel [7]. The solid residue is made of coke and ash, also known as char, and has little value as fuel.

Recently, the possibility of using char from pyrolysis of the plastic mixtures has been explored as a potential adsorbent [8]; however, the limited porosity compromises the potential of this solid as an adsorbent of metals in water, e.g., lead [9], among others [10]. Upgrading

the char by activation has proven to be an attractive strategy to prepare porous carbonaceous materials with outstanding adsorption properties for a wide range of pollutants in water, such as dyes [11], anthropogenic organic contaminants of emerging concern [12], or metals [13]. Physical and chemical activation has been demonstrated to be an extraordinary strategy for producing porous carbonaceous materials. The most efficient activation agents include the CO<sub>2</sub> atmosphere [14] as a physical method and NaOH or KOH under an inert atmosphere [15,16] as a chemical procedure.

Lead pollution in water can be ascribed to natural or artificial causes. Lead is one of the most hazardous contaminants, and its presence in drinking water is still a recurring problem around the world, especially in those countries that still use lead plumbing materials for water pipes or have not completely replaced them, such as the USA [17]. Lead pipes require careful corrosion control to prevent leaching into the aqueous media. Natural groundwater can also be polluted with lead due to close contact with ores [18]. In addition, lead can be present in the wastewater of many industries, including metal plating, paint, or battery storage industries [19]. Lead remediation can be performed using separation methods such as osmosis or adsorption. The use of adsorption is a convenient and affordable technology, accessible in many water treatment scenarios. Adsorption has been widely used due to the high efficiency of the removal from aqueous effluents and the diversity of materials to reach that purpose. Some examples of materials with high metal adsorption ability include carbonaceous materials [20,21], silica [22], zeolites [23], treated biomass [24], or metal-organic frameworks [25]. Using chars recycled from waste is a useful strategy to revalorize waste into a valuable material with metal adsorption properties [26]. The available data to date applied to lead adsorption is focused on the revalorization of biomass residues [27–32] or other wastes rich in carbon, such as tires [33–35], or mixtures of both [9,10].

This work focuses on the activation of a non-porous carbonaceous char obtained from the pyrolysis of a mixture of non-recyclable plastic waste. Different physical/chemical activators with basic character have been explored, i.e., CO<sub>2</sub>, NaOH, and KOH, comparing them to an N<sub>2</sub> blank test. The properties of the activated chars were assessed by N<sub>2</sub> adsorption isotherms, Scanning Electron Microscopy (SEM), Fourier Transformed Infrared Spectroscopy (FTIR), and Inductively Coupled Plasma Mass Spectroscopy (ICP-MS) for the analysis of the metal content. Also, the behavior of the solids as potential adsorbents was studied in terms of organic and inorganic carbon leaching, as well as metal lixiviation. The solids, due to their high basic character, were able to raise the pH of the solution after being suspended. Their ability to remove lead from an aqueous solution was evaluated, and the isotherms of adsorption were obtained and corrected concerning the precipitation contribution due to the pH rise.

## 2. Materials and Methods

### 2.1. Chemicals

Analytical grade chemicals (HCl, NaOH, and KOH) were acquired from Sigma-Aldrich® and used as received. Ultrapure water (18.2 MΩ·cm) from a Direct-Q®-UV system (Millipore®) was used in all the stock solutions preparation.

### 2.2. Synthesis of the Adsorbents from Pyrolysis Char and Characterization of the Solids

The char, namely “C”, was obtained from the pyrolysis of a mixture of plastics from non-selective collecting from a local urban solid waste processing plant. The average composition was rigid polypropylene (56%), high impact polystyrene (9%), expanded polystyrene (10%), and polyethylene and polypropylene film (25%). The pyrolysis was conducted under an N<sub>2</sub> atmosphere (100 L·min<sup>-1</sup>) at 500 °C for 90 min, with a 10 °C·min<sup>-1</sup> heating rate. The resulting char was ground and sieved, size below 500 μm. This char powder was stabilized by acid washing to remove ash and leachable components with an aqueous 1 M HCl solution (50 g·L<sup>-1</sup> of char) [36], followed by ultrapure water washing and drying step at 120 °C for 24 h. This stabilized char was labeled as “SC”.

Different chemical activation procedures were considered to turn the char into a porous carbonaceous solid. First, the activation of the char was carried out under a CO<sub>2</sub> atmosphere due to the good results provided by this technique in the literature [14]. Particularly, in the activation step, a gas flow rate of 100 mL·min<sup>-1</sup>, a temperature of 760 °C, a heating rate of 10 °C·min<sup>-1</sup>, and a hold time of 1 h were used. Then, the resulted material was stabilized with HCl, rinsed with water, and dried following the same procedure indicated above. This obtained material was named “SC-CO<sub>2</sub>”. Alternatively, chemical activation under an N<sub>2</sub> atmosphere (100 L·min<sup>-1</sup>) with the addition of NaOH and KOH (char: alkali ratio, 2:1 [37]) was carried out. In this case, for activation, a two-step process was adopted, including (i) heating from room temperature to 300 °C at 10 °C·min<sup>-1</sup> and holding at 300 °C for 1 h to ensure the melting of the alkali, and (ii) heating from 300 °C to 760 °C at 10 °C·min<sup>-1</sup> and then holding at 760 °C for 1 h. After the activation process, the material was stabilized with HCl, rinsed with water, and dried following the same procedure indicated above. The resulting activated carbons were named “SC-NaOH” and “SC-KOH” depending on the chemical agent used. Finally, a blank activation test was performed under an N<sub>2</sub> atmosphere under the same activation conditions as those used for SC-CO<sub>2</sub> preparation to analyze the influence of the physical and chemical agent, excluding the effect of thermal treatment, on the properties of the final product. The resulting material from this test was called SC-N<sub>2</sub>. Table S1 of the Supplementary Materials provides a summary of different prepared activated carbons.

The textural properties were assessed by N<sub>2</sub> adsorption–desorption isotherms at 77 K in an ASAP 2020 apparatus of Micromeritics®. The specific surface area was calculated by the BET method (S<sub>BET</sub>), the specific surface area of micropore (S<sub>MP</sub>) was estimated by the t-plot method, the total pore volume (V<sub>T</sub>) was calculated from the N<sub>2</sub> uptake at p/p<sub>0</sub> = 0.99, and the volume micropore (V<sub>MP</sub>) from the t-plot method. The morphology of the particles was evaluated by Scanning Electron Microscopy in a FEG-ESEM QUEMSCAN 650F device of FEI Quanta™. The presence of functional surface groups was studied by Fourier Transformed Infrared (FTIR) spectroscopy in a PerkinElmer® Spectrum 65 FT-IR device working within 550–4000 cm<sup>-1</sup>.

### 2.3. Adsorption Tests and Behavior of the Samples in Water

Batch adsorption tests were carried out in 100 mL Erlenmeyer flasks at room temperature (20 °C) containing Pb within 10–500 mg·L<sup>-1</sup> with an adsorbent dose of 0.5 g·L<sup>-1</sup> and 200 rpm stirring. According to previous studies of lead adsorption, the pH was set between 5 and 6. For pH adjustment, dropwise addition of NaOH or HCl solutions (1 or 0.1 M) was carried out. The pH was monitored in a Crison Basic 20 device. The lead adsorption isotherms were obtained after adsorbent–lead solution contact for 24 h, keeping constant the adsorbent dose. Aqueous samples were filtered with Nylon Filters (0.45 µm), and the concentration of Pb in water was obtained by Atomic Absorbance (AA) spectrometry in a PerkinElmer® PinAAcle 500 Flame device. Adsorption experiments were carried out in triplicate, and the average value was represented. The relative standard deviation was lower than 5%.

The pH at the point of zero charge (pH<sub>pzc</sub>) was determined by a standard acid–base titration method [38]. Briefly, solutions of 50 mL were prepared at different pH values between 2 and 11 by adding NaOH or HCl. Next, the solid was added at a dose of 0.5 g·L<sup>-1</sup> and kept under stirring until reaching a constant pH value. The pH<sub>pzc</sub> was obtained as the intersection of the curve of final versus initial pH with the bisector. The metal leaching of the solids was carried out at 3 different pH values, i.e., 3, 7, and 11, at a dose of 0.5 g·L<sup>-1</sup>. The metal present in the aqueous solution after 24 h of contact was analyzed in an Inductively Coupled Plasma Mass Spectrometry (ICP-MS) in a PerkinElmer® Optima8300 device, with samples filtered as mentioned above. The lixiviation degree of the whole metal content in the solid samples was determined by acid digestion according to standard EN 13656:2000. Moreover, the released Total Organic Carbon (TOC) and Inorganic Carbon (IC) in the water were analyzed in a Shimadzu® TOC-V<sub>CSH</sub> analyzer.

### 3. Results and Discussions

#### 3.1. Characterization of the Plastic Pyrolysis Char after Activation

The changes in the textural and porous properties were analyzed by N<sub>2</sub> adsorption-desorption isotherms; see results in Table 1. The char obtained from the pyrolysis of the mixture of plastics displayed a poor surface area, 15 m<sup>2</sup>·g<sup>-1</sup>. The stabilized char slightly raised the area to 19 m<sup>2</sup>·g<sup>-1</sup>, probably due to the removal of the ash content and leachable content. The activation of the SC led to a considerable increment in the surface area of the resulting materials. For example, the activation under a CO<sub>2</sub> atmosphere led to a material with 68 m<sup>2</sup>·g<sup>-1</sup>, poorly higher than the 49 m<sup>2</sup>·g<sup>-1</sup> value obtained under an inert N<sub>2</sub> atmosphere. A further area increment was produced by chemical activation under alkali presence. Thus, in the presence of NaOH, the resulting material developed a specific area of 247 m<sup>2</sup>·g<sup>-1</sup>. Highly enhanced results were obtained if KOH was used, leading to an almost doubled surface area, i.e., 487 m<sup>2</sup>·g<sup>-1</sup>. The N<sub>2</sub> isotherms depicted in Figure 1 performed a Type I according to IUPAC classification, characteristic of microporous materials. Furthermore, the H3 type hysteresis loops described during the desorption step, within relative pressures  $p/p_0 = 0.45-0.99$ , which features parallel branches that finally go up almost vertically, provide evidence of the presence of grove mesopores of non-rigid generation by flaky particles as described for other materials in the literature [39,40]. The microporosity percentage analysis of the samples followed a similar trend to the total BET surface area, in which the relative importance of microporosity assessed either in terms of surface or volume percentage followed the order SC-KOH > SC-NaOH > SC-CO<sub>2</sub> > SC-N<sub>2</sub>.

**Table 1.** Textural properties of the char from plastic pyrolysis before and after activation.

Sample	S <sub>BET</sub> (m <sup>2</sup> ·g <sup>-1</sup> )	S <sub>MP</sub> (m <sup>2</sup> ·g <sup>-1</sup> )	S <sub>MP</sub> /S <sub>BET</sub> (%)	V <sub>T</sub> (cm <sup>3</sup> ·g <sup>-1</sup> )	V <sub>MP</sub> (cm <sup>3</sup> ·g <sup>-1</sup> )	V <sub>MP</sub> /V <sub>T</sub> (%)
C	15	1	5.4	0.025	-	-
SC	19	18	92.2	0.040	0.036	90.0
SC-N <sub>2</sub>	45	6	12.6	0.082	0.003	3.0
SC-CO <sub>2</sub>	68	18	26.9	0.094	0.008	9.2
SC-NaOH	247	185	74.9	0.217	0.084	38.9
SC-KOH	487	414	85.0	0.300	0.180	60.0

S<sub>BET</sub>: specific surface area; S<sub>MP</sub>, specific surface area of micropore; S<sub>EXT</sub>: specific external surface area; V<sub>T</sub>: total pore volume; V<sub>MP</sub>: volume of micropore.

Microporosity is expected to be produced as a consequence of the reaction of the alkali, e.g., NaOH or KOH, with the carbon and oxygen in the char, which enhances the gasification reaction and release of CO and CO<sub>2</sub>. Moreover, the corresponding alkali carbonates (Na<sub>2</sub>CO<sub>3</sub> or K<sub>2</sub>CO<sub>3</sub>) and oxides (Na<sub>2</sub>O or K<sub>2</sub>O) promote the reaction at dynamic sites in the carbonaceous material, leading to the generation of plenty of porous channels [41]. If the efficiency of the two alkalis is compared, KOH has been reported to be more efficient than NaOH in producing a larger amount of micropores [16,42,43], which explains the larger porosity obtained for SC-KOH. This boosted porosity has been linked to the thermodynamics of the reaction between the alkali and carbon. The temperature required to trigger the reaction is lower in the case of KOH [44].

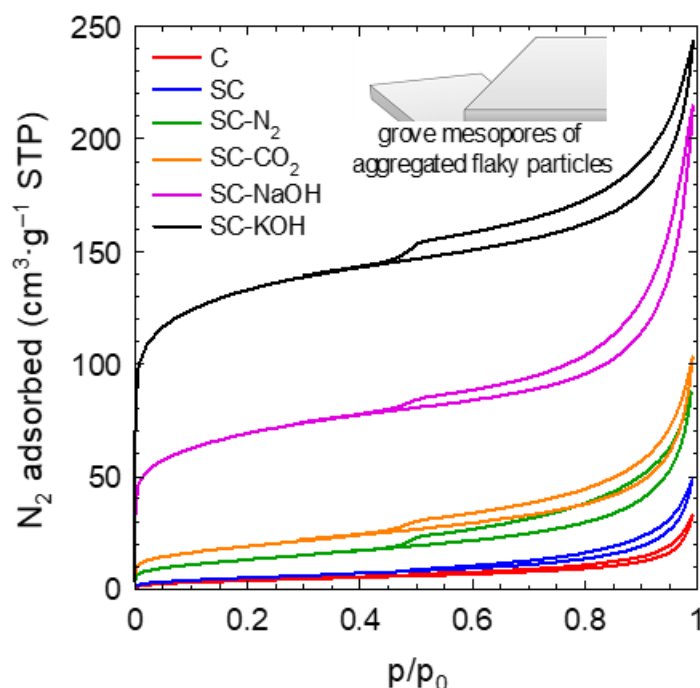


**Figure 1.**  $N_2$  adsorption–desorption isotherms of the char from plastic pyrolysis before and after activation.

The morphology of the particles was assessed by SEM. Micrographs of the char before and after activation are depicted in Figure 2. Despite the high heterogeneity of the char produced after pyrolysis, a consequence of the heterogeneity of the rejected plastic mixture, the SEM depicted micrographs suggested the presence of irregular flakes with low roughness onto the surface. These images support the already deduced morphology of the mesoporous described during the hysteresis desorption loop of  $N_2$  isotherms, as flaky aggregates are easily recognized. Compared to the native char, the stabilization after HCl washing and the latter thermal treatment is likely to increase the superficial irregularities, not as much as those monitored after chemical activation, though. Thus, the thermal chemical activation with  $CO_2$ , NaOH, or KOH considerably produced microscopic cavities and raised the imperfections of the surface [45], which explains the higher porosity registered in these samples. This porosity development is mainly due to the release of excess gases, i.e., CO and  $CO_2$ , during the activation process [41].

The composition of the superficial chemical groups of all the samples was assessed by FTIR in general terms analysis due to the complexity of the mixture pyrolyzed. The results are depicted in Figure 3. An important modification of the chemical structure can be observed after the chemical activation of the native char. The original char displayed broad-band of maximum ca.  $3400\text{ cm}^{-1}$ , which is attributed to superficial hydroxyl moiety [46]. After the stabilization with HCl, the  $-OH$  groups were completely removed. No signals corresponding to aliphatic groups of aliphatic hydrocarbons of alkanes or alkenes, peaks that should appear within  $2800\text{--}3000\text{ cm}^{-1}$  [47], were detected. The peaks at  $1600\text{ cm}^{-1}$  and  $1700\text{ cm}^{-1}$  were assigned to aromatic  $C=O$  and aromatic  $COOH/C=O$  stretching, respectively [47]. These oxygenated groups considerably decreased in intensity after stabilization with HCl washing and practically disappeared after thermal chemical activation. Moreover, a doubled peak characteristic of n-ring  $C=C$  stretch and conjugated  $C=C$  stretch (around  $1400\text{ cm}^{-1}$ ) [46] were well defined in the original char and also were partially destroyed during HCl washing and, finally, almost depleted after thermal treatment. The  $C-O-C$  peak located at  $\sim 1300\text{ cm}^{-1}$ , which was not observed in the original char, is linked to stretching mode in acids, ethers, and esters [48], increasing its intensity in the stabilization process with HCl to almost disappear after chemical activation. Finally, in the region of lowest wavelength values, a peak located at  $880\text{ cm}^{-1}$  appeared due to the presence of  $C-H$  of methyl groups or  $C-H$  out-of-plane bend [49]. In this case, after chemical activation, a

small definition of this peak can be observed. Also, the aromatic C-H was registered in the original char at around  $750\text{ cm}^{-1}$  [50], lowering the intensity after the stabilization and disappearing after the thermal treatment displayed an important intensity after the stabilization with HCl. The thermal treatment led to the decrease in this peak in the sample treated with  $\text{N}_2$ , and it was not observed after chemical activation in the rest of the samples. In summary, it can be deduced that the thermal treatment was mainly responsible for the removal of all the characteristic groups, especially the oxygenated ones.

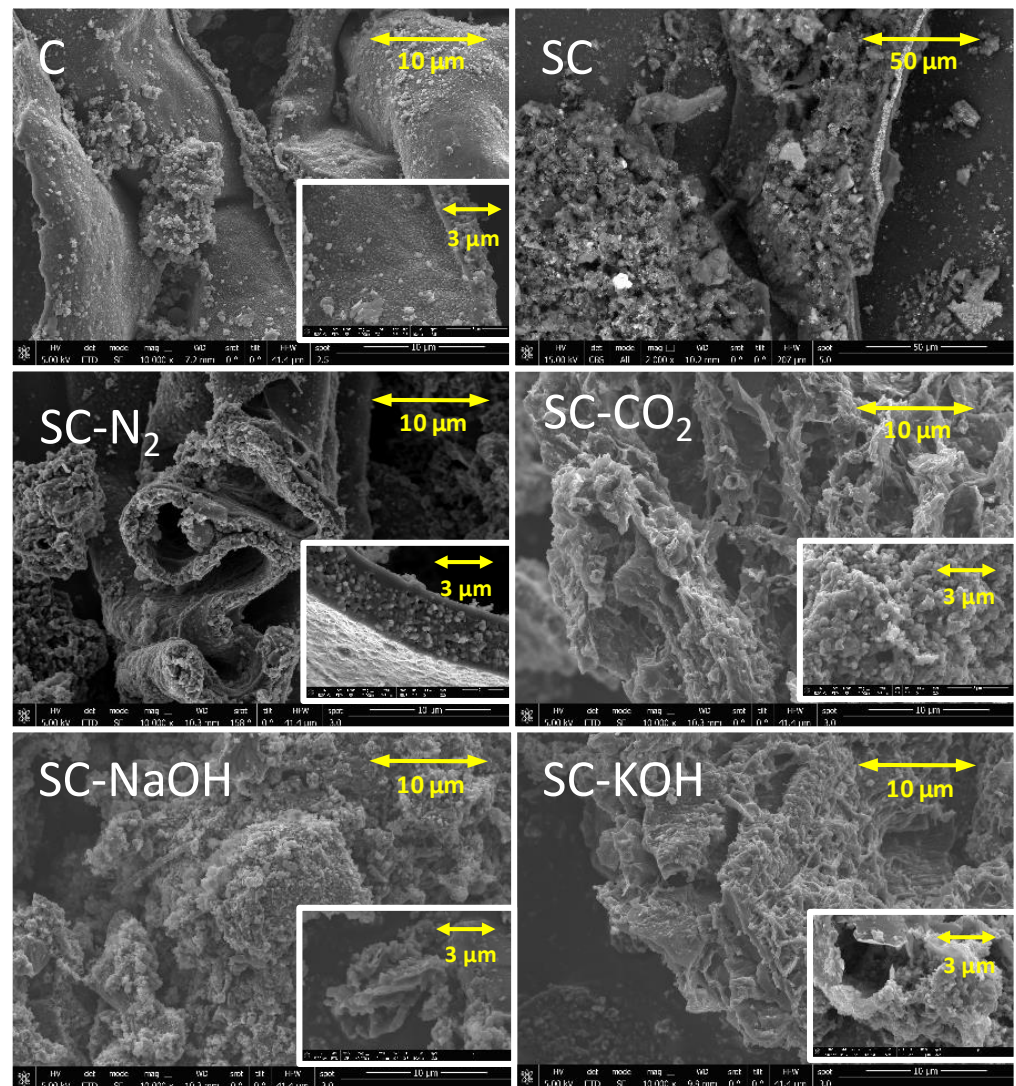


**Figure 2.** SEM micrographs of the char from plastic pyrolysis before and after activation.

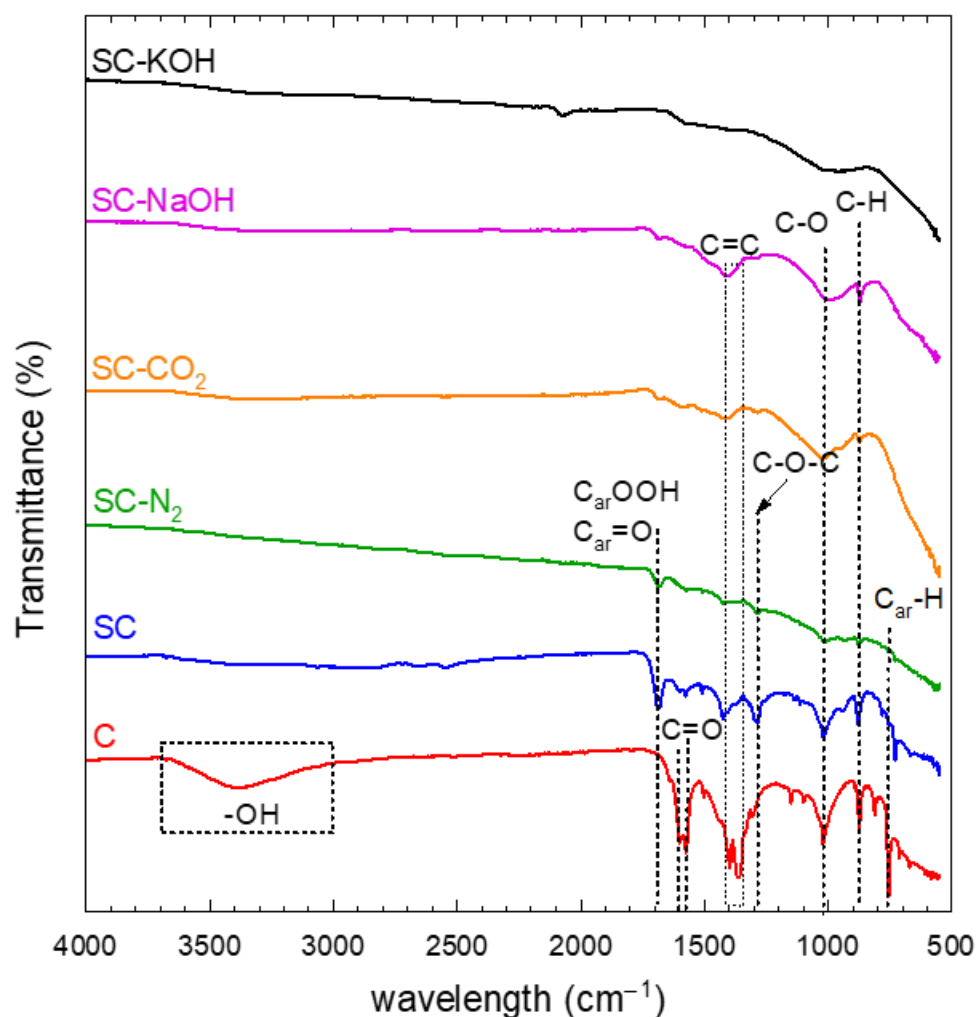


**Figure 3.** FTIR spectra of the char from plastic pyrolysis before and after activation.

The metallic composition of the solid samples before and after activation is summarized in Table 2. Diverse metals have historically been used in plastic production, either as pigments or stabilizers. As observed in Table 2, the concentration of metals in the solids was in the ppb range, except for Ti, Zn, Ba, and Sb, which raised until the ppm level, which is consistent with what has also been reported in the characterization of plastics [51,52] and pyrolyzed plastics chars [8]. The presence of a relevant amount of Ti is expected since  $\text{TiO}_2$  is overwhelmingly used as a white pigment [53]. ZnO and  $\text{Sb}_2\text{O}_3$  are also frequently used as multifunctional additives, not only due to their pigmentation properties but also as flame retardants or due to their fungicide abilities [52]. Barium sulfate is frequently added as an inert filler to increase the stiffness and hardness of plastics [52]. If the amount of Ti, Zn, Ba, and Sb are compared among the samples, a raising tendency in terms of concentration tendency of the metals after stabilization and chemical activation in which temperature is raised to 760 °C can be seen due to the slight mass loss during the chemical activation, keeping the metallic content in the final solid.

**Table 2.** Metallic composition ( $\text{mg}\cdot\text{kg}^{-1}$ ) of the char from plastic pyrolysis before and after activation.

Element	C	SC	SC-N <sub>2</sub>	SC-CO <sub>2</sub>	SC-NaOH	SC-KOH
Li	14	16	29	28	10	8
Ti	43,249	59,395	55,978	106,635	48,744	49,696
V	17	18	26	37	13	66
Cr	281	555	749	1221	453	1457
Mn	220	174	341	663	348	701
Co	8	11	8	39	8	14
Ni	192	318	231	1152	269	462
Cu	275	302	350	1095	163	173
Zn	2331	1791	303	29,109	5126	134
Ga	42	78	134	35	59	45
Se	0	0	0	1	0	0
Rb	17	18	27	18	6	17
Sr	383	204	236	145	400	254
Mo	13	22	23	143	12	13
Cd	1	1	0	0	0	0
Sn	78	63	49	120	52	44
Sb	182	2492	2369	3230	2430	8832
Ba	928	1786	3012	683	1282	826
W	10	124	14	48	39	18
Hg	0	1	0	1	0	0
Pb	457	487	132	453	189	36

### 3.2. Stability and Pb Adsorption of the Activated Pyrolysis Plastic Char in Water

The behavior in terms of stability, e.g., plausible leaching of organic matter and metals, of the activated char in the aqueous solution is very important due to the given potential application, i.e., as an adsorbent of contaminants in water. Accordingly, special attention was paid to the possible lixiviation of metals and organic and inorganic carbon. As the pH of the aqueous media is highly relevant to adsorption processes, the leaching effect was assessed at 3 different pH values, i.e., 3, 7, and 11.

The organic content released in water was considerably diminished after thermal chemical activation, see Figure 4. The original char from the pyrolysis of the plastics performed the highest TOC release, over  $120 \text{ mg}\cdot\text{L}^{-1}$ , which supposes 12% of the mass content. However, the HCl stabilization considerably reduced this effect, although still high for an application as an adsorbent; in this SC sample, an important effect on the pH was observed, with a higher TOC release when increasing the pH. The thermal and chemical activation dramatically diminished the TOC leached, being minimal, below ca.  $1 \text{ mg}\cdot\text{L}^{-1}$ . The release of IC was also diminished with HCl stabilization and chemical activation, leaching IC below  $3 \text{ mg}\cdot\text{L}^{-1}$ . Generally, a proportional increase of IC with pH was observed due to the formation of carbonates. However, NaOH was an exception with the IC lixiviated, approx.  $22 \text{ mg}\cdot\text{L}^{-1}$  independently of the pH.



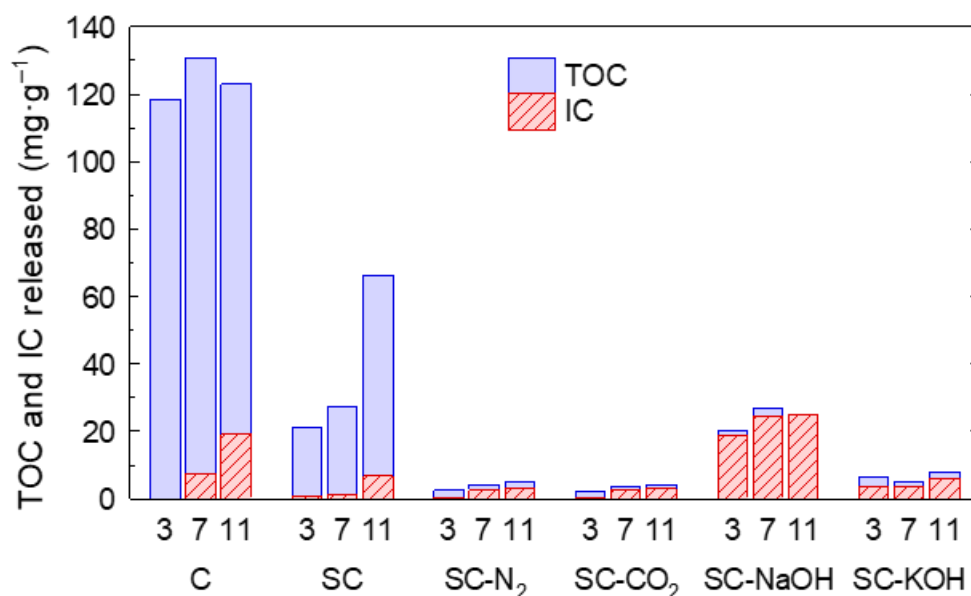


**Figure 4.** Organic and inorganic leaching of the char from plastic pyrolysis before and after activation at different pH values. Experimental conditions:  $C_{\text{solid}} = 1 \text{ g}\cdot\text{L}^{-1}$ ; time contact, 24 h.

The release of the leached metals during the contact of the solid samples was analyzed by measuring the metals in the aqueous solution normalized by the maximum content of metals in the solid samples. The results are represented in Figure 5. Among the metals with the highest contribution, as the previously provided analysis of the composition of the samples, Ti and Zn were not detected in the aqueous solution, probably due to the stability of their oxides, in all the pH tested [54,55]. Sb and Ba appeared in moderate concentration in the solids, and less than 10% was released in the original char, the stabilized, and the thermal treated with N<sub>2</sub> and CO<sub>2</sub>. The chemical activation with NaOH and KOH led to samples that were more stable in this sense. From the rest of the metals detected in the solid, Cu and Ni, which appeared in the solids at minor concentrations, were not detected in the leaching tests. Figure 5 shows important leaching, in terms of percentage, of Mo and W; however, it should be considered that the concentration of these metals is low in the solids, range of ppb. The most hazardous metals detected in the solid samples, Cd, Hg, and Pb, were at very low concentrations. The release of Cd was undetectable in the samples with potential application as adsorbents, e.g., SC-NaOH and SC-KOH. Aqueous Hg and Pb were not registered in any sample.

pH is one of the most important variables to study in adsorption processes due to the high influence it may have during the application of this technology. The behavior of the solid regarding the pH in an aqueous solution was evaluated by the determination of the  $\text{pH}_{\text{pzc}}$ . Figure 6 shows the results obtained for each sample. In general terms, the samples displayed a basic character, except for SC and SC-N<sub>2</sub>. The sample SC represents the char after HCl stabilization, which explains the acidic value for  $\text{pH}_{\text{pzc}}$  below 2. However, the sample SC-N<sub>2</sub> can be assumed as neutral with no significant change in pH observed in the tests, so the surface could be considered barely neutral. The activation with CO<sub>2</sub>, NaOH, and KOH led in all the cases to activated carbonaceous materials with a strong basic character describing an order SC-NaOH > SC-KOH > SC-CO<sub>2</sub>. The behavior of the SC-NaOH was remarkably outstanding, able to raise the pH of the aqueous medium to pH~11, whatever the initial pH was.

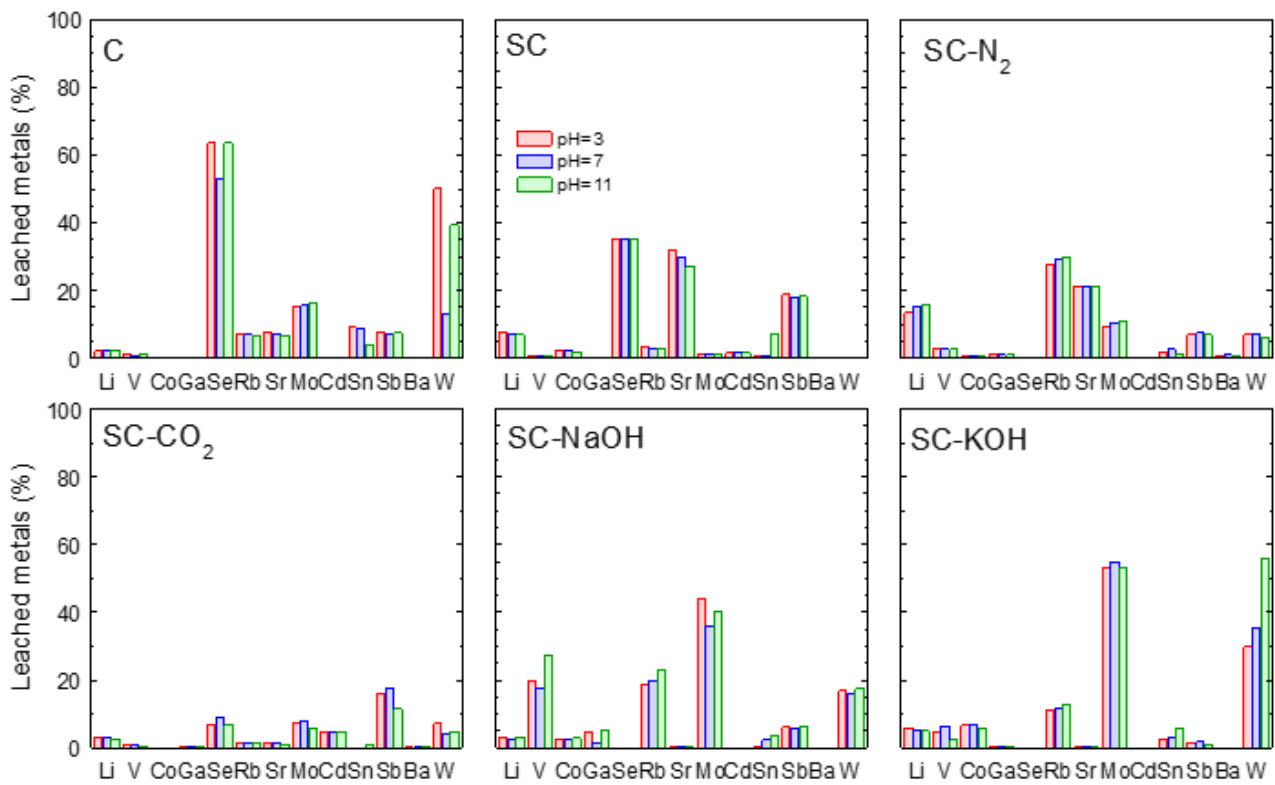


Figure 5. Metal leaching in the char from pyrolysis before and after activation at different pH.

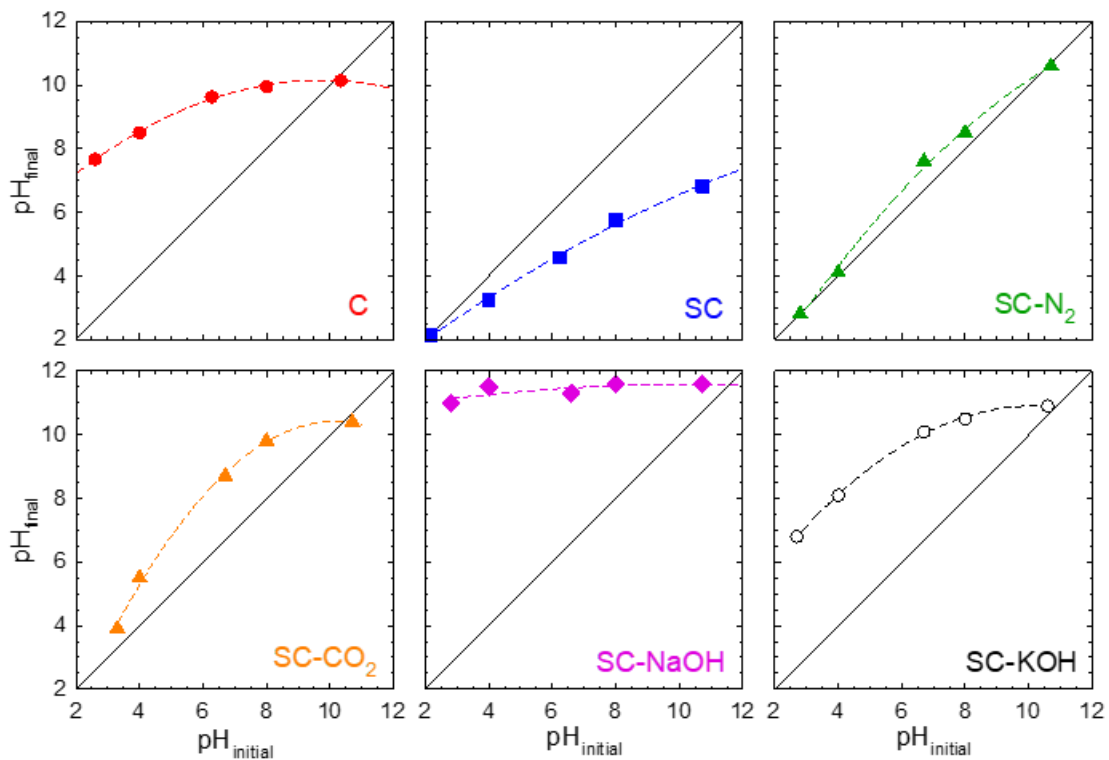
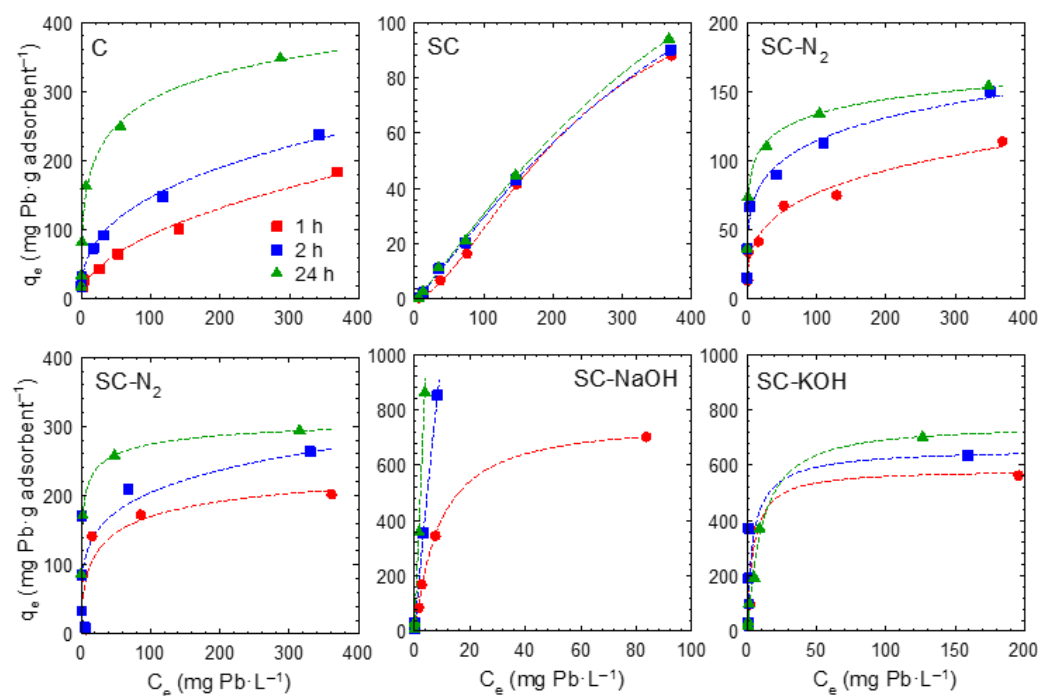


Figure 6. Determination of the  $pH_{pzc}$  by the drift method of the char from plastic pyrolysis before and after activation.

The adsorption isotherms were obtained for each sample, taking samples at 3 different times, 1 h, 2 h, and 24 h, i.e., equilibrium conditions. The results are displayed in Figure 7. If the adsorption performances are compared, the following adsorption capacity order is

observed: SC-NaOH > SC-KOH > C > SC-CO<sub>2</sub> > SC-N<sub>2</sub> > SC. The original char displayed a moderate adsorption capacity; however, its direct application lacks interest, and a stabilization step via washing is required to remove the highly easily released organic carbon. The stabilized sample, SC, led to the lowest adsorption performance, but the treatment was efficient in removing the release of undesirable organic matter. The activation with CO<sub>2</sub> and N<sub>2</sub> raised the adsorption ability concerning the SC sample; nevertheless, it was still insufficient to reach the results obtained with the native char. The chemical activation with NaOH and KOH considerably improved the adsorption results, leading to the solids with the highest adsorption capacities, especially in the case of NaOH activation. Nonetheless, the pH evolution during these experiments was a crucial variable since over pH = 6.0, according to the acid-base equilibria, the Pb<sup>2+</sup> ions start to precipitate as Pb(OH)<sub>2</sub> [56], resulting in the adsorption results initially registered being overestimated. This phenomenon has been reported in the literature with adsorbents that display a strong basic character, contributing to a precipitation mechanism of Pb rather than removal by adsorption of the ions onto the surface of the solid [57]. Figure 8 shows the variation of the pH for each solid depending on the initial Pb concentration tested. As depicted in this figure, the samples that were more affected by the pH rise and, therefore, by the precipitation phenomena were those with a strong basic character, i.e., SC-CO<sub>2</sub>, SC-NaOH, and SC-KOH, with SC-NaOH the sample with the highest contribution of precipitation as the final pH was not lower than 6.9 with the maximum Pb concentration tested. As previously shown in Figure 6, the sample SC-NaOH had a very strong basic acid character. Accordingly, a blank test to assess the precipitation contribution was carried out in the absence of solid, but adjusting the pH to the values registered during the equilibrium adsorption for each concentration tested. The removal monitored by precipitation was used to correct the adsorption capacities isotherms, as shown in Table 3. Low lead concentrations were highly affected by the precipitation effect specially in adsorption tests performed by SC-N<sub>2</sub>, SC-CO<sub>2</sub>, SC-NaOH, and SC-KOH. Only the SC sample did not show precipitation of lead since the pH of the liquid–solid suspension was between 4 and 5 for all concentrations tested.



**Figure 7.** Adsorption isotherms of Pb onto the char from plastic pyrolysis before and after activation. The dashed lines represent the fitting to the Sips isotherm model. Experimental conditions:  $C_{Pb0} = 10\text{--}500\text{ mg L}^{-1}$ ;  $C_{\text{adsorbent}} = 0.5\text{ g}\cdot\text{L}^{-1}$ ;  $T = 20\text{ }^{\circ}\text{C}$ .

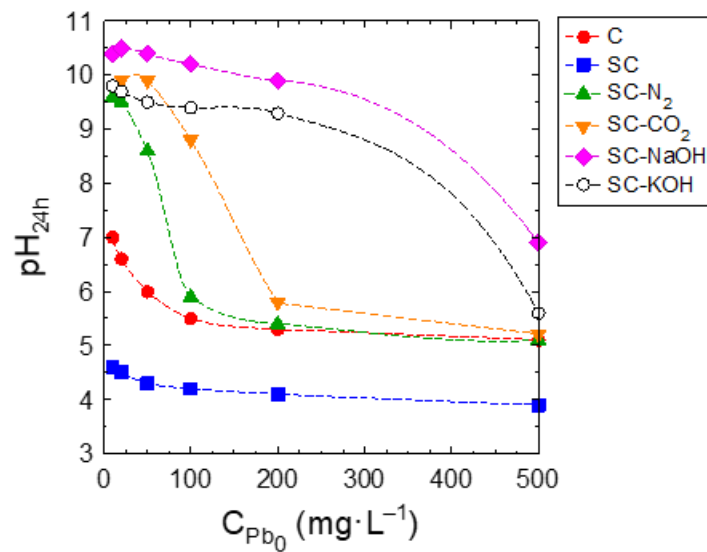


Figure 8. Evolution of the adsorption equilibria pH with the initial concentration of Pb.

Table 3. Experimental adsorption capacities and corrected adsorption capacities after precipitation.

Sample	q <sub>e</sub> (mg·g <sup>-1</sup> )	C <sub>i</sub> (mg·L <sup>-1</sup> )					
		10	20	50	100	200	500
C	Experimental	18.78	34.00	82.56	163.2	248.8	348.0
	Corrected	13.95	27.02	82.56	163.2	248.8	348.0
SC	Experimental	0.602	2.801	11.41	21.61	44.80	94.05
	Corrected	0.602	2.801	11.41	21.61	44.80	94.05
SC-N <sub>2</sub>	Experimental	15.64	36.56	73.60	117.2	124.1	154.0
	Corrected	0.537	1.427	16.92	117.2	124.1	154.0
SC-CO <sub>2</sub>	Experimental	19.26	34.42	85.88	171.5	247.6	294.0
	Corrected	0.709	1.298	3.758	22.03	243.2	294.0
SC-NaOH	Experimental	9.001	31.38	85.60	170.3	357.6	862.4
	Corrected	0.373	1.129	3.859	31.19	94.64	315.8
SC-KOH	Experimental	20.32	33.72	98.98	193.4	371.8	701.0
	Corrected	0.011	0.215	2.187	35.30	82.51	701.0

Different models frequently used in liquid phase adsorption were checked, i.e., the two-parameter models of Freundlich [58] and Langmuir [59] and the three-parameter Sips' model [60]. Table 4 summarizes the fitting results of each model for the case of equilibria conditions after subtracting the contribution of precipitation. Freundlich's model produced, in general terms, the worst fitting results in those samples in which the saturation level was close to being reached. The Freundlich equation considers that the energy of adsorption on a homogeneous surface is independent of surface coverage, making it impossible to predict the maximum adsorption capacity [61]. Langmuir's model, which implies the ideal assumptions of preferential monolayer coverage and energetic homogeneity of adsorption sites, fitted quite well to almost all the experimental series. The Sips model provided, in contrast, the best fitting results in all the samples. Sips' model is the result of a combination of both the Langmuir and Freundlich models, which is deduced to predict the heterogeneity of the adsorption systems as well as to circumvent the limitations associated with the increased concentrations of the adsorbate of the Freundlich model [62]. In turn, Sips leads

to the production of an expression that allows for predicting the saturation capacity at high concentrations, i.e., the  $q_s$  value shown in Table 4.

**Table 4.** Adsorption isotherm fittings after precipitation correction.

Sample	Model Parameters									
	Freundlich			Langmuir			Sips			
	$q_e = K_F C_e^{n_F}$			$q_e = K_L C_e^{n_F}$			$q_e = \frac{q_s (K_S C_e)^{n_S}}{1 + (K_S C_e)^{n_S}}$			
	$K_F$	$n_F$	$R^2$	$q_L$	$K_L$	$R^2$	$q_s$	$K_S$	$n_S$	$R^2$
C	97.45	0.227	0.975	318.8	0.175	0.938	594.8	$8.40 \times 10^{-3}$	0.371	0.979
SC	0.501	0.888	0.997	424.6	$7.77 \times 10^{-4}$	0.998	220.8	$2.11 \times 10^{-3}$	1.171	0.999
SC-N <sub>2</sub>	66.81	0.146	0.984	133.6	1.514	0.836	259.9	$1.26 \times 10^{-2}$	0.240	0.992
SC-CO <sub>2</sub>	139.7	0.137	0.951	271.1	1.148	0.869	334.0	0.448	0.400	0.999
SC-NaOH	221.2	1.201	0.999		N/A			N/A		
SC-KOH	109.9	0.388	0.939	767.7	$8.74 \times 10^{-2}$	0.989	746.7	$9.70 \times 10^{-2}$	1.107	0.990

$q_e$  (mg·g<sup>-1</sup>) is the Pb<sup>2+</sup> adsorbed at equilibrium;  $C_e$  (mg·L<sup>-1</sup>) is the remaining Pb<sup>2+</sup> concentration at equilibrium;  $K_F$  (mg<sup>1-n</sup>·g<sup>-1</sup>·L<sup>n</sup>) is the Freundlich constant;  $n_F$  (dimensionless) is the exponent of Freundlich's model;  $q_L$  (mg·g<sup>-1</sup>) is the Langmuir adsorption capacity;  $K_L$  (L·mg<sup>-1</sup>) is the Langmuir constant;  $q_s$  (mg·g<sup>-1</sup>) is the Sips adsorption capacity;  $K_S$  (L·mg<sup>-1</sup>) is the Sips constant;  $n_S$  (dimensionless) is the exponent of Sips' model.

In addition to extensively studied materials in the fields of wastewater treatment [22–25], several researchers have utilized the char of pyrolysis as a raw material to produce activated carbon and use it as an adsorbent of lead from aqueous solutions. Table 5 recompiles some of the published works. The production of activated carbon as an adsorbent of lead from aqueous solutions has been explored mainly from biomass wastes, with differences in the properties and lead adsorption capacities of produced activated carbons. The variability can be attributed mainly to differences in the composition of the raw materials but also the differences in pyrolysis and activation conditions. Although biomass is the main precursor to producing activated carbons from waste, the production of these adsorbents from tire waste or mixtures of biomass and plastics has also been reported in the literature. Regarding plastic waste, recently, Vieira et al. [63] and Wijesekara et al. [64] published complete reviews about the preparation methods for carbon-based materials from plastic waste. However, up to now, there have been very few reports about the conversion of plastic waste to activated carbon adsorbents for wastewater treatment [65–67]. From the results given in Table 5, it can be highlighted that the activated carbons produced from plastic waste are effective adsorbents for lead removal from wastewater since the adsorption capacities of SC-KOH (ca. 700 mg·g<sup>-1</sup>) was higher than many feedstocks reported in the literature. Therefore, plastic wastes could be used as alternative sources for the mass production of activated carbon.

**Table 5.** Some published works about lead adsorption by activated carbons obtained from char of pyrolysis of different precursors materials.

Type of Precursor	Raw Material	Activating Agent	Lead Adsorption Capacity (mg·g <sup>-1</sup> )	Refs.
Biomass	Black cumin seeds	H <sub>2</sub> SO <sub>4</sub>	18.0	[27]
	Banana peel	—	247.1	[28]
	Apricot stone	H <sub>2</sub> SO <sub>4</sub>	22.9	[29]
	Potato peel	H <sub>3</sub> PO <sub>4</sub> + KOH	9.3	[30]
	Coconut buttons	H <sub>2</sub> SO <sub>4</sub> + steam	92.7	[31]
	Soybean oil cake	K <sub>2</sub> CO <sub>3</sub>	476.2	[31]
	Olive stone	H <sub>3</sub> PO <sub>4</sub>	148.8	[32]
Tire waste		KOH	322.5	[33]
		Physical (agent not specified)	327.9	[34]
		KOH	49.7	[35]
Biomass and plastic waste	Bamboo, sugarcane, and neem PET, PE, and PVC	—	NA	[10]
Biomass, tire, and plastic waste	Forestry pine, used tires, and plastic wastes	—	1.87	[9]
Mixture of non-recyclable plastics	Polypropylene, polystyrene, and polyethylene	KOH	747	This work

#### 4. Conclusions

Plastics can be used as a source to prepare fuels, minimizing the impact of this waste that might otherwise end up in a landfill. The solid chars generated in the process can be considered a valuable carbonaceous source if activated for the preparation of porous materials with potential adsorption properties, such as the removal of metals in water. The original char displayed a moderate adsorption capacity (over 300 mg·g<sup>-1</sup>) but displayed considerable leaching of organic matter, which indicates its usefulness as a plausible adsorbent. Among the thermal chemical activation methods tested, i.e., thermal treatment in the presence of CO<sub>2</sub>, NaOH, and KOH, the use of KOH resulted in the most beneficial procedure for developing a porous structure with enhanced microporosity and potential adsorption of lead in water, with a maximum adsorption capacity of ca. 700 mg·g<sup>-1</sup>. Langmuir's model fitted quite well to almost all the experimental series. The Sips model provided, in contrast, the best fitting results in all the samples. All the activated carbon materials displayed a remarkable basic character in aqueous solution; as a consequence, low lead concentrations were highly affected by the precipitation effect, especially in adsorption tests performed by SC-NaOH, which contributed to the removal of lead mostly by precipitation due to the rise in pH.

**Supplementary Materials:** The following supporting information can be downloaded at: <https://www.mdpi.com/article/10.3390/app12168032/s1>, Table S1. Summary of experimental conditions used for the preparation of the different activated carbons.

**Author Contributions:** Conceptualization, M.Á.M.-L., G.B. and M.C.; methodology, J.B. and G.B.; software, R.R.S.; validation, R.R.S., M.Á.M.-L. and M.C.; formal analysis, R.R.S., M.Á.M.-L. and M.C.; investigation, A.L., J.B. and G.B.; resources, G.B.; data curation, R.R.S.; writing—original draft preparation, R.R.S., M.Á.M.-L. and M.C.; writing—review and editing, all authors; supervision, M.Á.M.-L. and M.C.; project administration, M.Á.M.-L., G.B. and M.C.; funding acquisition, M.Á.M.-L. and M.C. All authors have read and agreed to the published version of the manuscript.

**Funding:** This work has received funding from the project P20\_00167 (FEDER/Junta de Andalucía-Ministry of Economy, Transformation, Industry, and Universities) and the project B-RNM-78-UGR20 (FEDER/Junta de Andalucía-Ministry of Economic Transformation, Industry, and Universities). The authors are also grateful for the supporting analyses provided by the external services of the University of Granada (CIC) and the University of Málaga (SCAI).

**Institutional Review Board Statement:** Not applicable.

**Informed Consent Statement:** Not applicable.

**Data Availability Statement:** Data sharing not applicable.

**Conflicts of Interest:** The authors declare no conflict of interest.

## References

1. Plastics Europe Plastics—The Facts. 2021. Available online: <https://plasticseurope.org/knowledge-hub/plastics-the-facts-2021/> (accessed on 11 April 2022).
2. Martín-Lara, M.A.; Godoy, V.; Quesada, L.; Lozano, E.J.; Calero, M. Environmental status of marine plastic pollution in Spain. *Mar. Pollut. Bull.* **2021**, *170*, 112677. [[CrossRef](#)]
3. OECD Global Plastics Outlook. Available online: <https://www.oecd.org/environment/plastics/> (accessed on 10 May 2022).
4. Miandad, R.; Rehan, M.; Nizami, A.-S.; Abou, M.; Barakat, E.-F.; Ismail, I.M.; Miandad, R.; El-Fetouh Barakat, M.A.; Rehan, A.M.; Nizami, A.-S. The Energy and Value-Added Products from Pyrolysis of Waste Plastics. In *Recycling of Solid Waste for Biofuels and Bio-Chemicals*; Springer: Singapore, 2016; pp. 333–355.
5. Qureshi, M.S.; Oasmaa, A.; Pihkola, H.; Deviatkin, I.; Tenhunen, A.; Mannila, J.; Minkkinen, H.; Pohjakallio, M.; Laine-Ylijoki, J. Pyrolysis of plastic waste: Opportunities and challenges. *J. Anal. Appl. Pyrolysis* **2020**, *152*, 104804. [[CrossRef](#)]
6. Papari, S.; Bamdad, H.; Berruti, F. Pyrolytic Conversion of Plastic Waste to Value-Added Products and Fuels: A Review. *Materials* **2021**, *14*, 2586. [[CrossRef](#)] [[PubMed](#)]
7. Harussani, M.M.; Sapuan, S.M.; Rashid, U.; Khalina, A.; Ilyas, R.A. Pyrolysis of polypropylene plastic waste into carbonaceous char: Priority of plastic waste management amidst COVID-19 pandemic. *Sci. Total Environ.* **2022**, *803*, 149911. [[CrossRef](#)] [[PubMed](#)]
8. Martín-Lara, M.; Piñar, A.; Ligeró, A.; Blázquez, G.; Calero, M. Characterization and Use of Char Produced from Pyrolysis of Post-Consumer Mixed Plastic Waste. *Water* **2021**, *13*, 1188. [[CrossRef](#)]
9. Bernardo, M.; Mendes, S.; Lapa, N.; Gonçalves, M.; Mendes, B.; Pinto, F.; Lopes, H.; Fonseca, I. Removal of lead (Pb<sup>2+</sup>) from aqueous medium by using chars from co-pyrolysis. *J. Colloid Interface Sci.* **2013**, *409*, 158–165. [[CrossRef](#)]
10. Singh, E.; Kumar, A.; Mishra, R.; You, S.; Singh, L.; Kumar, S.; Kumar, R. Pyrolysis of waste biomass and plastics for production of biochar and its use for removal of heavy metals from aqueous solution. *Bioresour. Technol.* **2021**, *320*, 124278. [[CrossRef](#)]
11. Maneerung, T.; Liew, J.; Dai, Y.; Kawi, S.; Chong, C.; Wang, C.-H. Activated carbon derived from carbon residue from biomass gasification and its application for dye adsorption: Kinetics, isotherms and thermodynamic studies. *Bioresour. Technol.* **2016**, *200*, 350–359. [[CrossRef](#)] [[PubMed](#)]
12. Gómez-Avilés, A.; Peñas-Garzón, M.; Belver, C.; Rodríguez, J.J.; Bedia, J. Equilibrium, kinetics and breakthrough curves of acetaminophen adsorption onto activated carbons from microwave-assisted FeCl<sub>3</sub>-activation of lignin. *Sep. Purif. Technol.* **2021**, *278*, 119654. [[CrossRef](#)]
13. Sultana, M.; Rownok, M.H.; Sabrin, M.; Rahaman, M.H.; Alam, S.N. A review on experimental chemically modified activated carbon to enhance dye and heavy metals adsorption. *Clean. Eng. Technol.* **2022**, *6*, 100382. [[CrossRef](#)]
14. Murillo, R.; Navarro, M.V.; López, J.M.; García, T.; Callén, M.S.; Aylón, E.; Mastral, A.M. Activation of pyrolytic tire char with CO<sub>2</sub>: Kinetic study. *J. Anal. Appl. Pyrolysis* **2004**, *71*, 945–957. [[CrossRef](#)]
15. Bazargan, A.; Hui, C.W.; McKay, G. Porous Carbons from Plastic Waste. In *Advances in Polymer Science*; Springer LLC: New York, NY, USA, 2013; Volume 266, pp. 1–26.
16. Almazán-Almazán, M.C.; Perez-Mendoza, M.; López-Domingo, F.J.; Fernández-Morales, I.; Domingo-García, M.; López-Garzón, F.J. A new method to obtain microporous carbons from PET: Characterisation by adsorption and molecular simulation. *Microporous Mesoporous Mater.* **2007**, *106*, 219–228. [[CrossRef](#)]
17. Schweitzer, L.; Noblet, J. Water Contamination and Pollution. In *Green Chemistry: An Inclusive Approach*; Elsevier: Amsterdam, The Netherlands, 2018; pp. 261–290. ISBN 9780128095492.
18. Mushak, P. Lead in the Human Environment: Fate and Transport Processes. In *Trace Metals and Other Contaminants in the Environment*; Elsevier: Amsterdam, The Netherlands, 2011; Volume 10, pp. 91–115.
19. Kumar, V.; Dwivedi, S.K.; Oh, S. A critical review on lead removal from industrial wastewater: Recent advances and future outlook. *J. Water Process Eng.* **2022**, *45*, 102518. [[CrossRef](#)]
20. Goel, J.; Kadirvelu, K.; Rajagopal, C.; Garg, V.K. Removal of lead(II) by adsorption using treated granular activated carbon: Batch and column studies. *J. Hazard. Mater.* **2005**, *125*, 211–220. [[CrossRef](#)] [[PubMed](#)]
21. Momčilović, M.; Purenović, M.; Bojić, A.; Zarubica, A.; Randelović, M. Removal of lead(II) ions from aqueous solutions by adsorption onto pine cone activated carbon. *Desalination* **2011**, *276*, 53–59. [[CrossRef](#)]

22. Li, S.; Li, S.; Wen, N.; Wei, D.; Zhang, Y. Highly effective removal of lead and cadmium ions from wastewater by bifunctional magnetic mesoporous silica. *Sep. Purif. Technol.* **2021**, *265*, 118341. [[CrossRef](#)]
23. Baker, H.M.; Massadeh, A.M.; Younes, H. Natural Jordanian zeolite: Removal of heavy metal ions from water samples using column and batch methods. *Environ. Monit. Assess.* **2008**, *157*, 319–330. [[CrossRef](#)] [[PubMed](#)]
24. Mohammadabadi, S.I.; Javanbakht, V. Fabrication of dual cross-linked spherical treated waste biomass/alginate adsorbent and its potential for efficient removal of lead ions from aqueous solutions. *Ind. Crop. Prod.* **2021**, *168*, 113575. [[CrossRef](#)]
25. Far, H.S.; Hasanzadeh, M.; Najafi, M.; Nezhad, T.R.M.; Rabbani, M. Efficient Removal of Pb(II) and Co(II) Ions from Aqueous Solution with a Chromium-Based Metal–Organic Framework/Activated Carbon Composites. *Ind. Eng. Chem. Res.* **2021**, *60*, 4332–4341. [[CrossRef](#)]
26. Liu, M.; Almatrafi, E.; Zhang, Y.; Xu, P.; Song, B.; Zhou, C.; Zeng, G.; Zhu, Y. A critical review of biochar-based materials for the remediation of heavy metal contaminated environment: Applications and practical evaluations. *Sci. Total Environ.* **2022**, *806*, 150531. [[CrossRef](#)] [[PubMed](#)]
27. Thabede, P.M.; Shooto, N.D.; Naidoo, E.B. Removal of methylene blue dye and lead ions from aqueous solution using activated carbon from black cumin seeds. *South Afr. J. Chem. Eng.* **2020**, *33*, 39–50. [[CrossRef](#)]
28. Ahmad, Z.; Gao, B.; Mosa, A.; Yu, H.; Yin, X.; Bashir, A.; Ghozeisi, H.; Wang, S. Removal of Cu(II), Cd(II) and Pb(II) ions from aqueous solutions by biochars derived from potassium-rich biomass. *J. Clean. Prod.* **2018**, *180*, 437–449. [[CrossRef](#)]
29. Kobya, M.; Demirbas, E.; Senturk, E.; Ince, M. Adsorption of heavy metal ions from aqueous solutions by activated carbon prepared from apricot stone. *Bioresour. Technol.* **2005**, *96*, 1518–1521. [[CrossRef](#)] [[PubMed](#)]
30. Osman, A.I.; Blewitt, J.; Abu-Dahrieh, J.K.; Farrell, C.; Al-Muhtaseb, A.H.; Harrison, J.; Rooney, D.W. Production and characterisation of activated carbon and carbon nanotubes from potato peel waste and their application in heavy metal removal. *Environ. Sci. Pollut. Res.* **2019**, *26*, 37228–37241. [[CrossRef](#)] [[PubMed](#)]
31. Anirudhan, T.S.; Sreekumari, S.S. Adsorptive removal of heavy metal ions from industrial effluents using activated carbon derived from waste coconut buttons. *J. Environ. Sci.* **2011**, *23*, 1989–1998. [[CrossRef](#)]
32. Bohli, T.; Ouederni, A.; Fiol, N.; Villaescusa, I. Single and binary adsorption of some heavy metal ions from aqueous solutions by activated carbon derived from olive stones. *Desalin. Water Treat.* **2015**, *53*, 1082–1088. [[CrossRef](#)]
33. Shahrokhi-Shahraki, R.; Benally, C.; El-Din, M.G.; Park, J. High efficiency removal of heavy metals using tire-derived activated carbon vs commercial activated carbon: Insights into the adsorption mechanisms. *Chemosphere* **2021**, *264*, 128455. [[CrossRef](#)] [[PubMed](#)]
34. Gupta, V.K.; Ganjali, M.R.; Nayak, A.; Bhushan, B.; Agarwal, S. Enhanced heavy metals removal and recovery by mesoporous adsorbent prepared from waste rubber tire. *Chem. Eng. J.* **2012**, *197*, 330–342. [[CrossRef](#)]
35. Nieto-Márquez, A.; Pinedo-Flores, A.; Picasso, G.; Atanes, E.; Kou, R.S. Selective adsorption of Pb<sup>2+</sup>, Cr<sup>3+</sup> and Cd<sup>2+</sup> mixtures on activated carbons prepared from waste tires. *J. Environ. Chem. Eng.* **2017**, *5*, 1060–1067. [[CrossRef](#)]
36. Bernardo, M.; Lapa, N.; Gonçalves, M.; Mendes, B.; Pinto, F.; Fonseca, I.M.F.L.; Lopes, H. Physico-chemical properties of chars obtained in the co-pyrolysis of waste mixtures. *J. Hazard. Mater.* **2012**, *219–220*, 196–202. [[CrossRef](#)] [[PubMed](#)]
37. Lian, F.; King, B.; Zhu, L. Comparative study on composition, structure, and adsorption behavior of activated carbons derived from different synthetic waste polymers. *J. Colloid Interface Sci.* **2011**, *360*, 725–730. [[CrossRef](#)] [[PubMed](#)]
38. Lopez-Ramon, M.V.; Stoeckli, F.; Moreno-Castilla, C.; Carrasco-Marin, F. On the characterization of acidic and basic surface sites on carbons by various techniques. *Carbon* **1999**, *37*, 1215–1221. [[CrossRef](#)]
39. Sing, K.S.W.; Everett, D.H.; Haul, R.A.W.; Moscou, L.; Pierotti, R.A.; Rouquerol, J.; Siemieniewska, T. Reporting physisorption data for gas/solid systems with special reference to the determination of surface area and porosity. *Pure Appl. Chem.* **1985**, *57*, 603–619. [[CrossRef](#)]
40. Thommes, M.; Kaneko, K.; Neimark, A.V.; Olivier, J.P.; Rodriguez-Reinoso, F.; Rouquerol, J.; Sing, K.S. Physisorption of gases, with special reference to the evaluation of surface area and pore size distribution (IUPAC Technical Report). *Pure Appl. Chem.* **2015**, *87*, 1051–1069. [[CrossRef](#)]
41. Kaur, B.; Gupta, R.K.; Bhunia, H. Chemically activated nanoporous carbon adsorbents from waste plastic for CO<sub>2</sub> capture: Breakthrough adsorption study. *Microporous Mesoporous Mater.* **2019**, *282*, 146–158. [[CrossRef](#)]
42. Yuan, X.; Lee, J.G.; Yun, H.; Deng, S.; Kim, Y.J.; Lee, J.E.; Kwak, S.K.; Lee, K.B. Solving two environmental issues simultaneously: Waste polyethylene terephthalate plastic bottle-derived microporous carbons for capturing CO<sub>2</sub>. *Chem. Eng. J.* **2020**, *397*, 125350. [[CrossRef](#)]
43. Muniandy, L.; Adam, F.; Mohamed, A.R.; Ng, E.-P. The synthesis and characterization of high purity mixed microporous/mesoporous activated carbon from rice husk using chemical activation with NaOH and KOH. *Microporous Mesoporous Mater.* **2014**, *197*, 316–323. [[CrossRef](#)]
44. Lillo-Ródenas, M.A.; Cazorla-Amorós, D.; Linares-Solano, A. Understanding chemical reactions between carbons and NaOH and KOH: An insight into the chemical activation mechanism. *Carbon* **2003**, *41*, 267–275. [[CrossRef](#)]
45. Hussin, F.; Aroua, M.K.; Kassim, M.A.; Ali, U.F. Transforming Plastic Waste into Porous Carbon for Capturing Carbon Dioxide: A Review. *Energies* **2021**, *14*, 8421. [[CrossRef](#)]
46. Suriapparao, D.V.; Ojha, D.; Ray, T.; Vinu, R. Kinetic analysis of co-pyrolysis of cellulose and polypropylene. *J. Therm. Anal. Calorim.* **2014**, *117*, 1441–1451. [[CrossRef](#)]



47. Xue, Y.; Zhou, S.; Brown, R.C.; Kelkar, A.; Bai, X. Fast pyrolysis of biomass and waste plastic in a fluidized bed reactor. *Fuel* **2015**, *156*, 40–46. [[CrossRef](#)]
48. Foo, K.Y.; Hameed, B.H. Utilization of biodiesel waste as a renewable resource for activated carbon: Application to environmental problems. *Renew. Sustain. Energy Rev.* **2009**, *13*, 2495–2504. [[CrossRef](#)]
49. Singh, R.K.; Ruj, B.; Sadhukhan, A.K.; Gupta, P. A TG-FTIR investigation on the co-pyrolysis of the waste HDPE, PP, PS and PET under high heating conditions. *J. Energy Inst.* **2020**, *93*, 1020–1035. [[CrossRef](#)]
50. Li, C.; Ataei, F.; Atashi, F.; Hu, X.; Gholizadeh, M. Catalytic pyrolysis of polyethylene terephthalate over zeolite catalyst: Characteristics of coke and the products. *Int. J. Energy Res.* **2021**, *45*, 19028–19042. [[CrossRef](#)]
51. Prunier, J.; Maurice, L.; Perez, E.; Gigault, J.; Wickmann, A.-C.P.; Davranche, M.; Ter Halle, A. Trace metals in polyethylene debris from the North Atlantic subtropical gyre. *Environ. Pollut.* **2019**, *245*, 371–379. [[CrossRef](#)]
52. Turner, A.; Filella, M. Hazardous metal additives in plastics and their environmental impacts. *Environ. Int.* **2021**, *156*, 106622. [[CrossRef](#)]
53. McKeen, L.W. Introduction to Plastics and Polymers. In *Permeability Properties of Plastics and Elastomers*; William Andrew Publishing: Norwich, NY, USA, 2017; pp. 21–40. ISBN 978-0-323-50859-9.
54. Lee, S.-Y.; Park, S.-J. TiO<sub>2</sub> photocatalyst for water treatment applications. *J. Ind. Eng. Chem.* **2013**, *19*, 1761–1769. [[CrossRef](#)]
55. Yebra, D.M.; Kiil, S.; Weinell, C.E.; Dam-Johansen, K. Dissolution rate measurements of sea water soluble pigments for antifouling paints: ZnO. *Prog. Org. Coat.* **2006**, *56*, 327–337. [[CrossRef](#)]
56. Liu, Q.; Liu, Y. Distribution of Pb(II) species in aqueous solutions. *J. Colloid Interface Sci.* **2003**, *268*, 266–269. [[CrossRef](#)]
57. Su, X.; Chen, Y.; Li, Y.; Li, J.; Song, W.; Li, X.; Yan, L. Enhanced adsorption of aqueous Pb(II) and Cu(II) by biochar loaded with layered double hydroxide: Crucial role of mineral precipitation. *J. Mol. Liq.* **2022**, *357*, 1198–1206.e12. [[CrossRef](#)]
58. Freundlich, H. Über die Adsorption in Lösungen. *Z. Phys. Chem.* **1907**, *57U*, 385–470. [[CrossRef](#)]
59. Langmuir, I. The adsorption of gases on plane surfaces of glass, mica and platinum. *J. Am. Chem. Soc.* **1918**, *40*, 1361–1403. [[CrossRef](#)]
60. Sips, R. On the Structure of a Catalyst Surface. *J. Chem. Phys.* **1948**, *16*, 490. [[CrossRef](#)]
61. Sparks, D.L. Sorption Phenomena on Soils. In *Environmental Soil Chemistry*, 2nd ed.; Academic Press: London, UK, 2003; ISBN 978-0-12-656446-4.
62. Al-Ghouti, M.A.; Da'Ana, D.A. Guidelines for the use and interpretation of adsorption isotherm models: A review. *J. Hazard. Mater.* **2020**, *393*, 122383. [[CrossRef](#)]
63. Vieira, O.; Ribeiro, R.S.; de Tuesta, J.L.D.; Gomes, H.T.; Silva, A.M. A systematic literature review on the conversion of plastic wastes into valuable 2D graphene-based materials. *Chem. Eng. J.* **2022**, *428*, 131399. [[CrossRef](#)]
64. Wijesekara, D.A.; Sargent, P.; Ennis, C.J.; Hughes, D. Prospects of using chars derived from mixed post waste plastic pyrolysis in civil engineering applications. *J. Clean. Prod.* **2021**, *317*, 128212. [[CrossRef](#)]
65. Mendoza-Carrasco, R.; Cuerda-Correa, E.M.; Alexandre-Franco, M.F.; Fernández-González, C.; Gómez-Serrano, V. Preparation of high-quality activated carbon from polyethyleneterephthalate (PET) bottle waste. Its use in the removal of pollutants in aqueous solution. *J. Environ. Manag.* **2016**, *181*, 522–535. [[CrossRef](#)]
66. Kumari, M.; Chaudhary, G.R.; Chaudhary, S.; Umar, A. Transformation of solid plastic waste to activated carbon fibres for wastewater treatment. *Chemosphere* **2022**, *294*, 133692. [[CrossRef](#)]
67. Ilyas, M.; Ahmad, W.; Khan, H. Utilization of activated carbon derived from waste plastic for decontamination of polycyclic aromatic hydrocarbons laden wastewater. *Water Sci. Technol.* **2021**, *84*, 609–631. [[CrossRef](#)]